IEEE Access
Multidisciplinary ⋮ Rapid Review ⋮ Open Access Journal

Received 13 November 2022, accepted 3 December 2022, date of publication 9 December 2022,
date of current version 19 December 2022.

Digital Object Identifier 10.1109/ACCESS.2022.3228110

RESEARCH ARTICLE

A Novel Circular Reconfigurable Metasurface-Based Compact UWB Hybrid Coupler for Ku-Band Applications

MOHAMED ATEF ABBAS[1,2], MEHMET FARUK CENGIZ[3], A.M.M.A. ALLAM[4], DIAA E. FAWZY[3], (Member, IEEE), HADIA M. ELHENNAWY[1], (Member, IEEE), AND MOHAMED FATHY ABO SREE[2]

[1]Department of Electronics and Communications Engineering, Ain Shams University, Cairo 11517, Egypt
[2]Department of Electronics and Communications Engineering, Arab Academy for Science, Technology and Maritime Transport, Cairo 451913, Egypt
[3]Faculty of Engineering, Izmir University of Economics, 35330 İzmir, Turkey
[4]Faculty of Information Engineering and Technology, German University, Cairo 101516, Egypt

Corresponding author: Mehmet Faruk Cengiz (mehmetfarukcengiz@gmail.com)

ABSTRACT A novel circular reconfigurable metasurface (MS) based compact ultra-wideband (UWB) hybrid coupler is developed for Ku-band applications. The coupler is developed using the substrate-integrated gap waveguide (SIGW) technology. The coupler structure consists of two layers, the bottom layer represents the artificial magnetic surface of the periodic structures and the ridges in between that guide the wave in the required direction with minimum dispersion. It involves the coupling section with a centered etched slot and two additional vias to achieve the basic hybrid coupler properties. This layer is nominated as the ridge layer. The second layer is a circular shape of a dielectric gap loaded with the top ground. The top ground is left solid for a non-reconfigurable coupler. Concerning the reconfigurable coupler, this layer contains an artificial metasurface of Jerusalem cross elements where the copper is etched around. This layer is nominated as the gap layer. This MS surface is mechanically rotated to offset the magnitude and phase of the signal going to the through and coupled ports. The findings obtained from the simulations show that the reconfiguration can be accomplished by rotating the MS around the source coupler's central axis. The rotation is tested between 0° to 180° in the counter-clockwise direction. The operating frequency range of the coupler is between 11.94 to 16.91 GHz, which covers approximately the whole Ku-band. The coupler delivers continuously adjustable amplitude between 2.6 and 4.8 dB while the phase differences within 77° to 105° over a fractional bandwidth (FBW) of 34.45%. It is manufactured using PCB technology and measured using network analyzer. A strong agreement is achieved between simulations and measurements. The proposed coupler can be used in traditional beam-forming and beam-steering networks by changing the rotation angle or the operating frequency. The developed coupler can replace the Butler and Bless matrices with their complication, heavy number of phase shifters, and crossover problems. The current work can be extended to operate in the mm-Wave band by changing the dimension and the material of the unit cell of the ridge layer of the coupler.

INDEX TERMS 3 dB hybrid coupler, gap waveguide, MS, tunable coupler, SIGW.

I. INTRODUCTION

Couplers with their numerous functionalities have received great attention in the development of multi-standard communication systems. The functions of signal isolation, mixing, and separation, as well as signal amplitude and phase

The associate editor coordinating the review of this manuscript and approving it for publication was Wanchen Yang.

acquisition, are vital for 5G and future 6G communication systems, making directional couplers critical components. At low-frequency bands, waveguides and microstrip couplers have achieved remarkable advancements in recent years. However, microstrip couplers encounter significant dielectric losses in the millimeter wave frequency region. In addition, standard metallic waveguide couplers suffer from difficulty in production, high costs and the ability to integrate with other networks. The operation at higher frequencies requires a suitable waveguide. Thus, gap waveguide (GW) technology has emerged as a potential replacement that could be employed in such bands without any of the aforementioned restrictions [1], [2]. As a result, many coupler designs have been studied using GW technology in recent years [3], [4], [5], [6], [7], [8], [9], [10], [11], [12], [13], [14], [15], [16]. However, none of them is reconfigurable.

The demands for reconfigurable devices are increasing because of the great flexibility and simple expansions they offer for new usage conditions. Moreover, the ability to reconfigure a wireless communication system has become a necessity to save costs and provide the best performance for various applications. Couplers are commonly used to build a beamforming network and produce the required radiation beams. A hybrid coupler, acting as a phase shifter, is also capable of performing a power division function and a phase shift. It is important to note that a typical coupler-based beamforming network can only produce limited beams because of the standard phase differences such as 90° and 0°/180°. But, it is typically required to have wide constantly controllable phase differences for greater flexibility. The easiest approach is to add a phase shifter after the power divider or the hybrid coupler. However, the following three major issues arise later: high insertion loss, significant phase change, and enormous circuit size [17]. The radiation beams can be constantly scanned over a large area if the coupler can give a reconfigurable phase difference. That is why it is essential to have a coupler with a broad phase adjustment range.

Reconfigurable couplers have garnered a lot of interest in microwave integrated circuits with variable power-dividing ratios [18], [19], [20], [21], and operating-frequency adjustment [22], [23], [24], [25]. Only a few numbers of structures have been documented in the literature since the reconfigurability in phase difference is more difficult than that in frequency or power division ratio [26], [27], [28], [29]. Varactor-tuned couplers were investigated to complete the continuously adjustable differential phase at a given frequency in order to increase the phase coverage. Generally, tuning ranges between 45° and 135° can be provided with the current phase-reconfigurable couplers. The periodic employment of varactors as transmission line loads allows control voltage modification of the equivalent circuit capacitance which supplies a 30°-150° phase difference [26]. In [27], a varactor-loaded branch line coupler ensures equal power division with a configurable phase difference of 45° to 135°. The implementation of an adjustable phase shifting unit for the horizontal branch can cause the phase difference to be continuously set from 45° to 135° [28]. In [29], a tunable unit was made up of open and shorted stubs, tunable capacitors, and two eighth wavelength linked lines which achieved a 0° to 180° phase difference. All the reported phase tunable capacitor designs are lumped elements based and their operating frequencies are mostly below 3 GHz.

In this study, a novel mechanically reconfigurable compact SIGW-based hybrid coupler is presented. A variation of adjustable amplitudes and phases are achievable by rotating the MS surface of the top layer.

The paper is arranged as follows: In Section II, the non-reconfigurable and MS tunable couplers are presented. In Section III, the performances of both couplers are discussed based on the experimentally validated results. Section IV concludes this article.

II. SIGW COUPLER DESIGN AND FABRICATION

A. SIGW DESIGN

Basically a gap waveguide is developed between two parallel conducting metallic plates, one of which has a textured surface made of pins or vias to produce a perfect magnetic conductor (PMC) surface. The other layer has a perfect electric conductor (PEC) on top of the structure. These two layers are separated by a gap height that is less than a quarter wavelength of the PMC plate. As a result, a stop band that prevents the parallel-plate modes from propagation can be achieved in the PMC-PEC cut-off zone. Metal ridges are interspersed between the textured plates to sustain the wave in a certain direction. The waveguide is created in a small space between the ridge and the top metallic plate, which is typically filled with air but in our work it is filled with a dielectric material which is known as substrate-integrated waveguides (SIGW). The SIGW has more advantages over ridge gap waveguide (RGW) with an air gap being replaced by a dielectric material as it maintains a constant gap height that minimizes the risk of possibility that this gap collapses in the presence of stress or impact. The fabrication process is also simpler (PCB-based). Another disadvantage of the RGW with an air-filled structure is that it requires very accurate CNC machining and its performance is unstable. Inside the gap, a quasi-TEM condition is maintained over the ridge and an electromagnetic (EM) leakage is stopped [30], [31]. So, our design is carried out based on SIGW technology.

Based on SIGW technology, the unit cell of the current design is composed of two parallel layers positioned as a bottom Rogers RO4350B ($\epsilon_r = 3.66$) and a top Rogers RO4003C ($\epsilon_r = 3.55$) substrates. In the bottom layer, the ground and the conductor mushroom patches are connected by vias. The directing ridge is positioned in the middle of the unit cells to activate the desired propagating quasi-TEM mode. Fig. 1 depicts the simulated dispersion diagram of the unit cell and supercell. The dispersion diagram of the unit cell covers the frequency range from 8.1 to 22.4 GHz as simulated by the CST Eigen Mode Solver. The frequency range of the supercell design is 8.6 to 22.1 GHz, and it is obvious

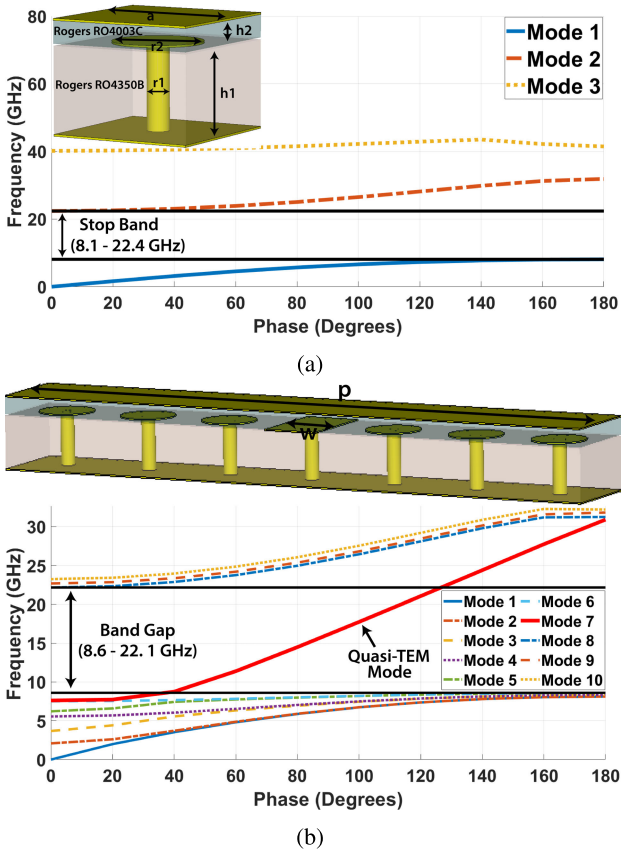

FIGURE 1. Dispersion diagram of a) unit cell b) supercell.

TABLE 1. Dimensions of the unit cell and supercell.

Parameters	p	r1	r2	a	h1	h2	w
Values (mm)	18.2	0.4	1.6	2.6	1.524	0.203	1.6

that the ridge lowers the stopband by approximately 5.6%. Fig. 2 demonstrates the feeding network of the proposed SIGW and the surface current distribution for two distinct frequencies, one is in the band and the other is out of the band. At 15 GHz, it is evident that the wave is constrained while leaking occurs at 5 GHz which is out of the band. Table 1 shows all the dimensions of the unit cell and supercell structures. It is determined that 1.6 mm is the optimal ridge width value. In essence, by adapting the strip line impedance equation, the characteristic impedance of the ridge can be determined. A small deviation from the results is predicted because the structure consists of two different substrates with close ϵ_r values.

For the measurement of the scattering parameters of the coupler, a standard RF edge SMA connector should be connected to the ridge which is difficult to be implemented. A transition shown in Fig.3 is designed for this purpose. A microstrip line of characteristic impedance of 50 Ω connects the ridge line to the SMA connector. The microstrip line is implemented on the top layer with a thickness of 0.45 mm and it contacts the upper surface of the ridge as shown in Fig. 3. Table 2 shows the microstrip transition dimensions.

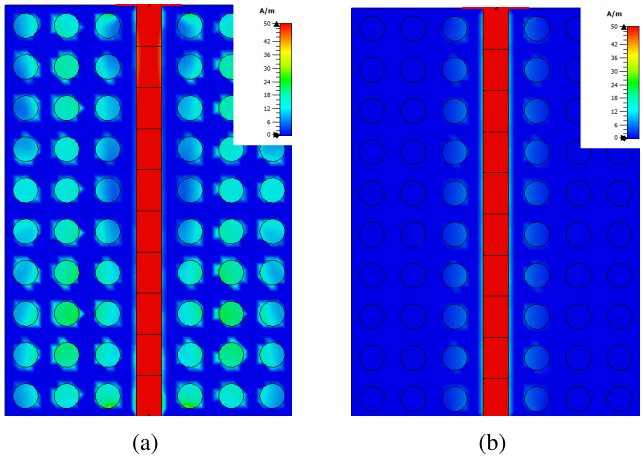

FIGURE 2. SIGW feeding network surface current distribution at (a) 5 GHz (b) 15 GHz.

TABLE 2. Dimensions of the microstrip-SIGW transition.

Parameters	t	l	f	g
Values (mm)	0.8	3.7	0.45	2.6

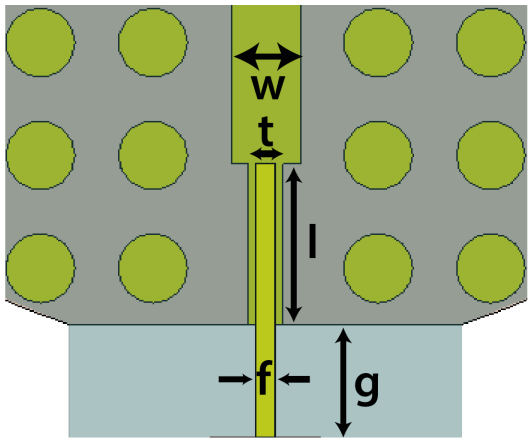

FIGURE 3. SIGW microstrip line transition.

TABLE 3. Dimensions of the new mm-Wave unit cell.

Parameters	b	r3	r4	h3	h4
Values (mm)	2.5	0.4	1	0.504	0.203

The bottom layer of the coupler is illustrated in Fig. 4, it contains four reciprocally coupled printed ridge gap waveguide (PRGW) lines. The coupling section is a circular junction patch with a 45° elliptical slot in the center of those lines. In addition, two more vias are added at an orthogonal angle to the slot axis. This slot and vias are intended for achieving a better power distribution in 3 dB hybrid coupler. This coupler's design is comparable to a typical microstrip or bulky wave couplers. According to the basic design concept [5] of the hybrid coupler, if two parallel lines have characteristic impedances of Z_0, the other two parallel lines should have impedances of $Z_0/\sqrt{2}$. The lengths L1 and L2 are not

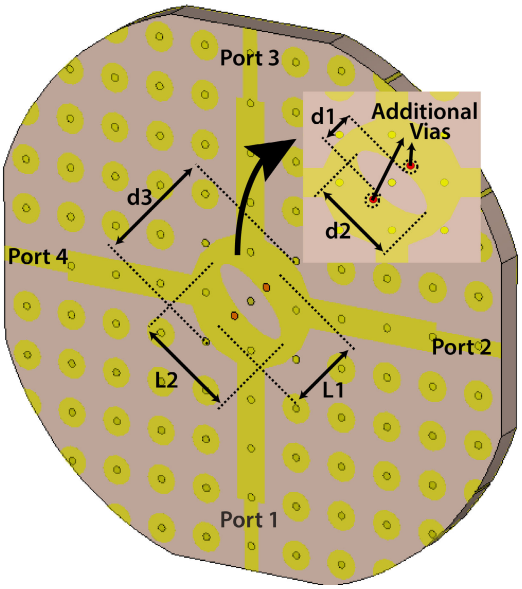

FIGURE 4. Bottom (Ridge) layer of the proposed coupler.

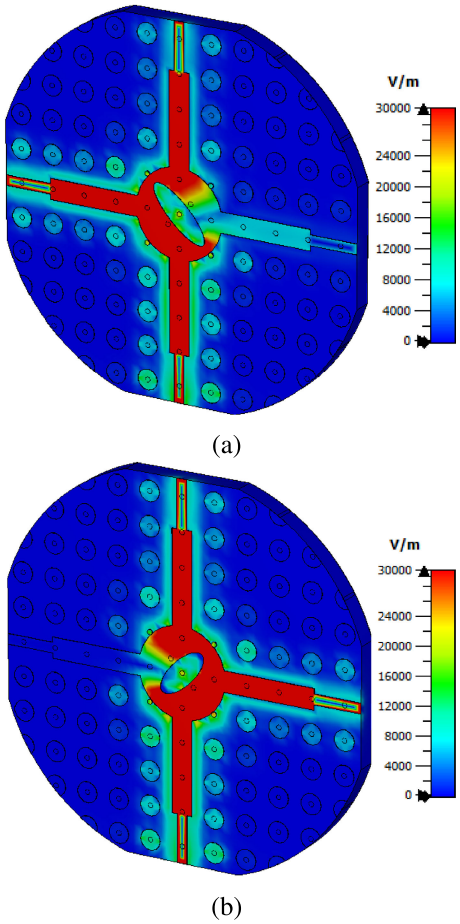

FIGURE 5. E-field distribution at 13.5 GHz. a) slot is left inclined b) slot is right inclined.

precisely identical to the $\lambda_g/4$ value, two correction factors are provided for designing the SIGW coupler effectively as

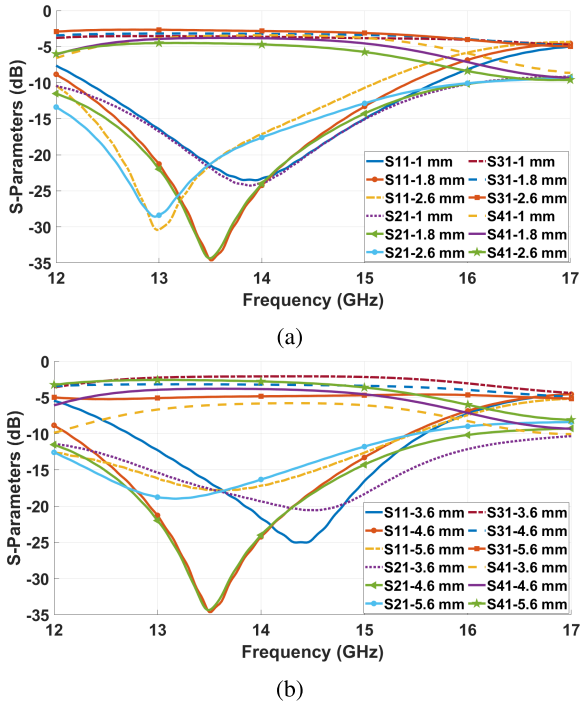

FIGURE 6. Simulated scattering parameters a) d1 variation b) d2 variation.

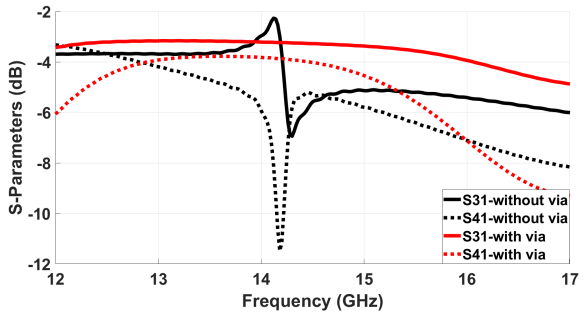

FIGURE 7. Effects of additional vias on the scattering parameters of the proposed coupler.

given by Eqs. 1,2.

$$L1 = (1 + b) \times (\lambda_g/4). \quad (1)$$

$$L2 = (1 + c) \times (\lambda_g/4). \quad (2)$$

where b and c represent two additional correction factors. The starting values of b and c can be set to zero, but the final values must be tuned depending on the optimal passband and the isolation performance. The optimum values for L1 and L2 are 3.1 mm and 5.8 mm, respectively. The elliptical slot's location specifies the isolation port to be used. The isolation is port 2 if the slot is slanted to the left; if it is inclined to the right, the isolation is port 4. Fig.5 demonstrates the electric field distribution in terms of elliptical slot placement. In order to improve the power distribution, two vias were also placed at the bottom of the circular patch. The optimized dimensions of the elliptical slot are $d1 = 1.8$ mm and $d2 = 4.6$ mm and the diameter of the circular patch

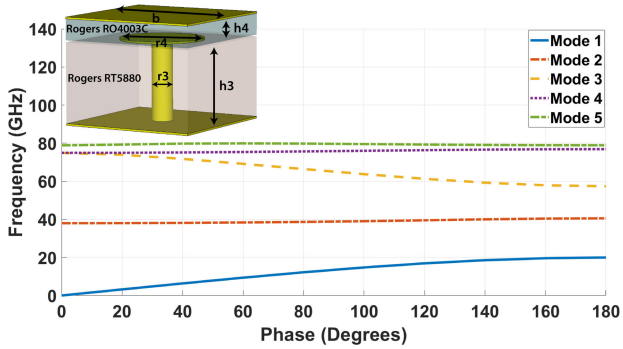

FIGURE 8. Dispersion diagram of the mm-Wave unit cell.

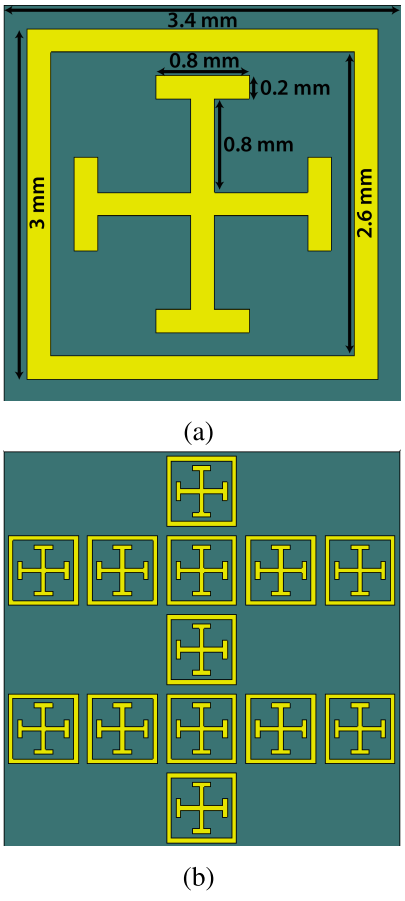

FIGURE 9. Proposed MS design a) Unit cell b) Metasurface.

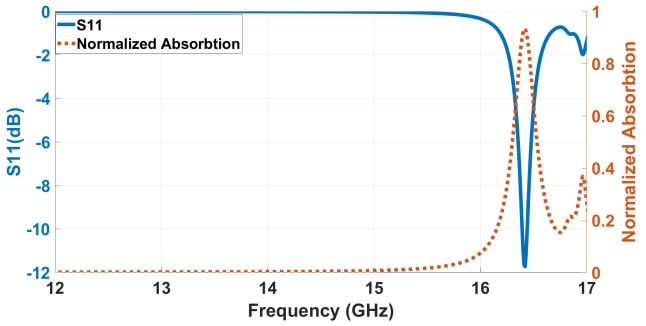

FIGURE 10. Simulated reflection coefficients and normalized absorption rates.

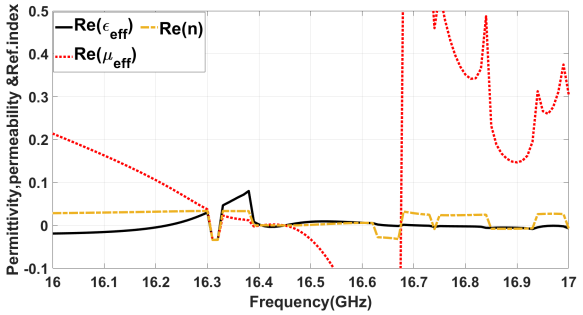

FIGURE 11. Calculated real part of relative permittivity, permeability and refractive index of the metasurface.

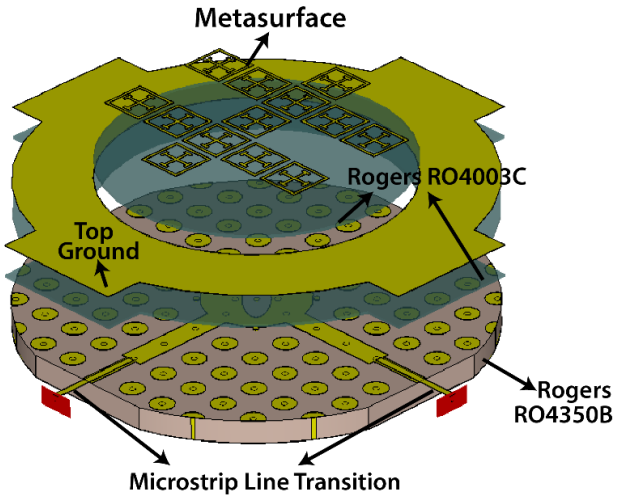

FIGURE 12. Proposed MS-based reconfigurable coupler.

$d3 = 7$ mm. The scattering parameter variations with the elliptical slot dimensions d1 and d2 are depicted in Fig. 6. It can be seen that the center frequency shifts depending on the size of the slot. The optimized values of d1 and d2 are obtained by changing one parameter while keeping the second one constant and vice versa. If d1 and d2 decrease, the center frequency shifts to higher frequencies. If d1 values increase, the shifting occurs at lower frequencies. An increase in the d2 does not affect the center frequency. The effects of additional vias in term of power division are shown in Fig.7. It is evident that huge losses occur between 14 GHz and 15 GHz without vias. Adding two extra vias helps in the equal power division. It is important to point out that this structure can be easily extended to operate in the mm-Wave band for 5G/6G applications. This can be achieved by the precise design of the unit cell of the ridge layer of the coupler as depicted in Fig. 8. This dispersion diagram shows that the artificial magnetic conductor (AMC) vias can generate a bandstop to accommodate a quasi-TEM mode over two subbands of mm-Wave applications with a BW more than 18 GHz. The material layer is changed to Rogers RT5880 and the dimension is changed according to the values in Table 3. It is considered for the future work of the current structure.

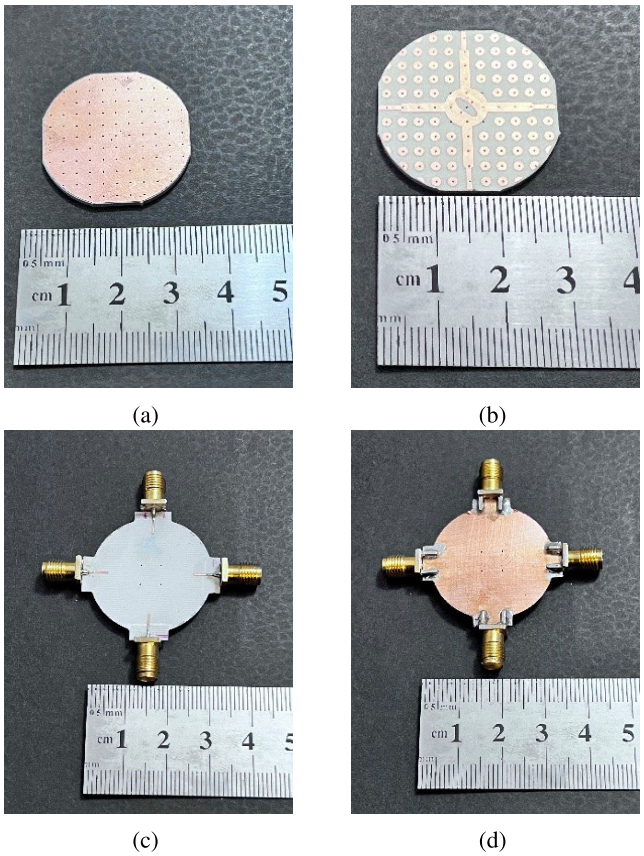

FIGURE 13. Fabricated coupler (without MS) a) bottom view of ridge layer b) top view of ridge layer c) bottom view of the gap layer d) top view of the gap layer.

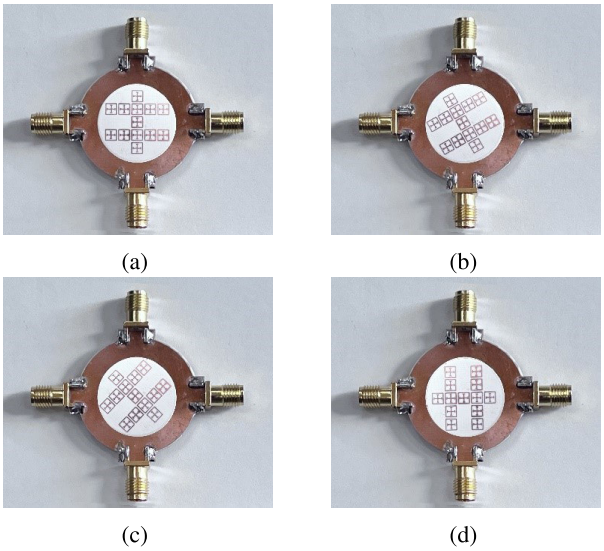

FIGURE 14. Fabricated reconfigurable coupler (with MS) at different rotated angles a) 0° b) 30° c) 45° d) 90°.

B. METASURFACE DESIGN

Fig. 9 demonstrates the Jerusalem cross-unit cell and the MS design. The finite size MS is investigated in order to determine its effective permittivity (ϵ_r), permeability (μ_r), reflection, transmission and absorption performances. The plane wave analysis is performed by the CST simulator.

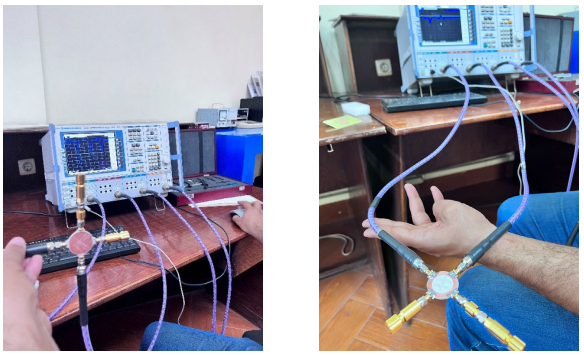

FIGURE 15. Measurement setup of proposed couplers using ROHDE & SCHWARZ ZVB20 vector network analyzer a) without reconfiguration b) reconfigurable coupler.

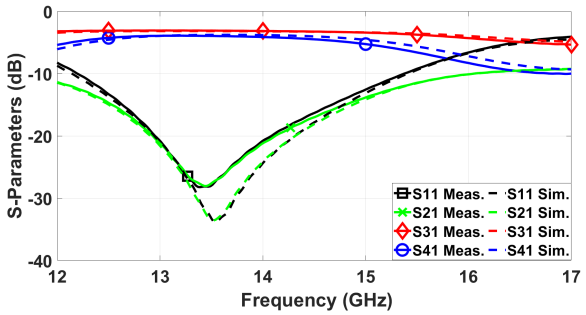

FIGURE 16. Scattering parameters of the coupler.

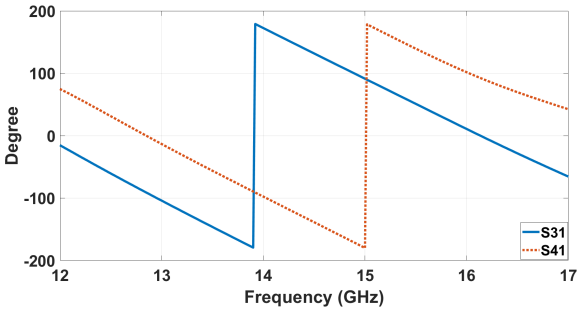

FIGURE 17. Phase responses of port 3 and port 4.

The basic formulas for the MS's equivalent impedance Z, the refractive index n, μ_r, and ϵ_r can be written as [32]:

$$Z = \pm\sqrt{\frac{(1+S_{11})^2 - S_{21}^2}{(1-S_{11})^2 - S_{21}^2}}. \tag{3}$$

$$X = 1/[2S_{21}(1/S_{11}^2 + S_{21}^2)]. \tag{4}$$

$$e^{jnk_0d} = X \pm j\sqrt{1-X^2}. \tag{5}$$

where k_0, d are the wave number and MS equivalent thickness, respectively.

$$\epsilon_r = Re\{n/Z\} \quad \text{and} \quad \mu_r = Re\{nZ\}. \tag{6}$$

The scattering parameters and the normalized absorption rates are shown in Fig.10. One can see that the MS behaves as

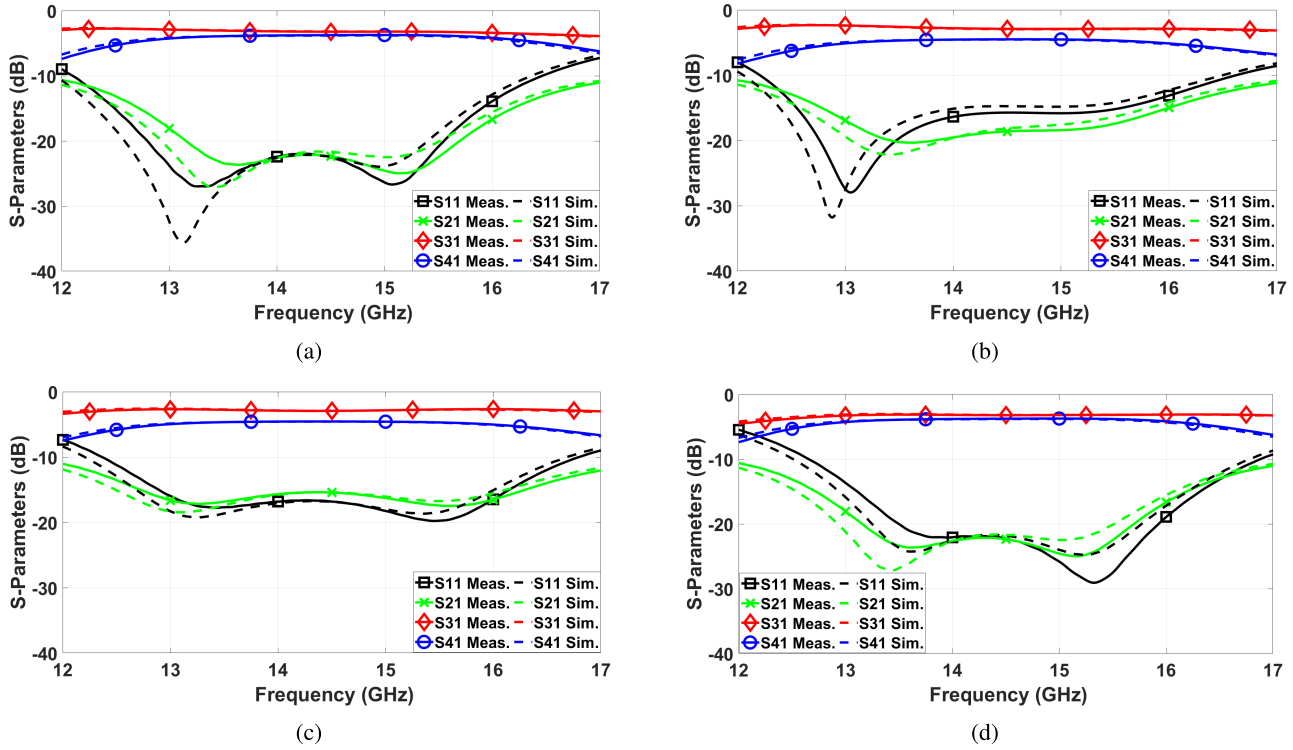

FIGURE 18. Scattering parameters of reconfigurable coupler at different angles a) 0° b) 30° c) 45° d) 90°.

a reflector over the whole operating frequency range except between 16 and 17 GHz, it is an absorber. In the frequency range from 16.4 to 16.7 GHz, the MS is a left-hand metasurface with a negative index of refraction n, negative μ_r, and negative ϵ_r values. It is a right-hand gap absorber from 16.7 up to 17 as shown in Fig. 11.

The proposed reconfigurable coupler design is based on Jerusalem cross MS as depicted in Fig.12. The top layer of the SIGW is circularly cut for the MS to be mechanically adjusted and rotated. The diameter of the rotating surface is 20 mm.

C. FABRICATED COUPLER

This section is devoted to the fabrication of the proposed coupler using PCB technology. Concerning the coupler structure, it is divided into two main layers. The gap layer includes the dielectric gap and top ground. The ridge layer comprises the vias, the ridge and the feeding network including the transition as depicted in Fig. 13. For the sake of reconfiguration the top ground of the gap layer includes a separate interior circular section of the MS structure which can be rotated for different angles as shown in Fig.14. Fig. 15 illustrates the measurement setup for measuring the scattering parameters of both couplers using network analyzer ROHDE & SCHWARZ ZVB20.

III. RESULTS AND DISCUSSION

Concerning the non-reconfigurable coupler, Fig. 16 depicts the simulated and measured scattering parameters of the proposed design. One notices that it operates 12.14 to 15.4 GHz under -10 dB level. Also, the coupling coefficients at port 3 and port 4 are nearly 3 dB with isolation at port 2. Fig. 17 shows the phases of the scattering parameters at ports 3 and 4. One can infer that the phase difference between them is nearly 90°. It is clear that the proposed coupler is a SIGW-based technology that achieves the hybrid parameters performance of the conventional couplers. The strong agreement between the measured results and the simulated ones validates all the new findings of the study.

Concerning the proposed reconfigurable coupler, the top MS layer is mechanically rotating in counter-clockwise directions to achieve different scattering parameters at ports 3 and 4. As shown in Fig.18 the reflection coefficient values vary with rotation keeping a persistent common frequency band. The widest bandwidth (UBW) occurs between 11.94 GHz to 16.91 GHz at 150° while the narrowest one is between 13.07 GHz to 16.34 GHz at 30°. The common BW among the different angles of incidence is approximately 4.2 GHz. The return loss is almost below -20 dB for all rotation angles. The isolation is greater than 15 dB for all cases. As can be observed, the two-output amplitude responses are slightly changing according to the rotation angle. The output power remains steady between 2.6 dB and 4.8 dB range in the middle as shown in Fig 19. However, the power fluctuates in port 4 at 8 dB at the corner of the operating frequency. As demonstrated in Fig. 20, one can notice that the phase variation at ports 3 and 4 cover the range from 180° to -180° keeping the phase difference between them ($\angle S_{41}$- $\angle S_{31}$) tunable in the range from 77° to 105°. The maximum phase

TABLE 4. Comparison between the proposed coupler and previous studies.

Ref.	Technology	Freq. (GHz)	FBW(%)	Return loss (dB)	Tuning types	Phase difference	Additional insertion loss (dB)
[13]	GGW	13-15	14.3	<-20	Non-tunable	90 ± 1	NA
[14]	PRGW	27.5-31.5	13	-23	Non-tunable	90 ± 5	NA
[15]	RGW	10.36-11.77	13	-34	Non-tunable	84°-94°	NA
[22]	Microstrip (MS)	2.1-2.45	15.2	<-20	Frequency	0°-10°	NA
[26]	Microstrip (Varactor)	2.2-2.75	31.6	<-10	Frequency & Phase	30°-150°	<1.4
[28]	Microstrip (Varactor)	0.9-1.1	20	<-10	Phase	45°-135°	<3
[29]	Microstrip (Varactor)	2.4 f_c	20	<-10	Phase	0°-180°	<2.2
This work	MS-based SIGW	11.94-16.91	34.45	<-20	Phase	77°-105°	<0.2

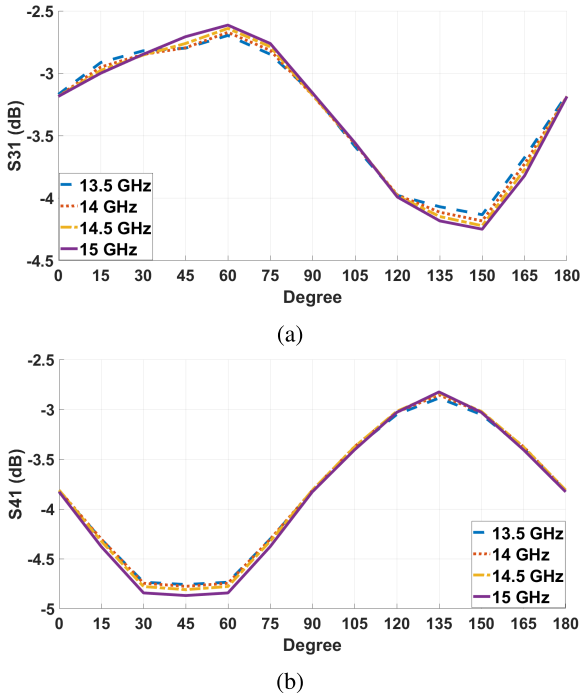

FIGURE 19. Response of rotation angle on output ports a) S_{31} b) S_{41}.

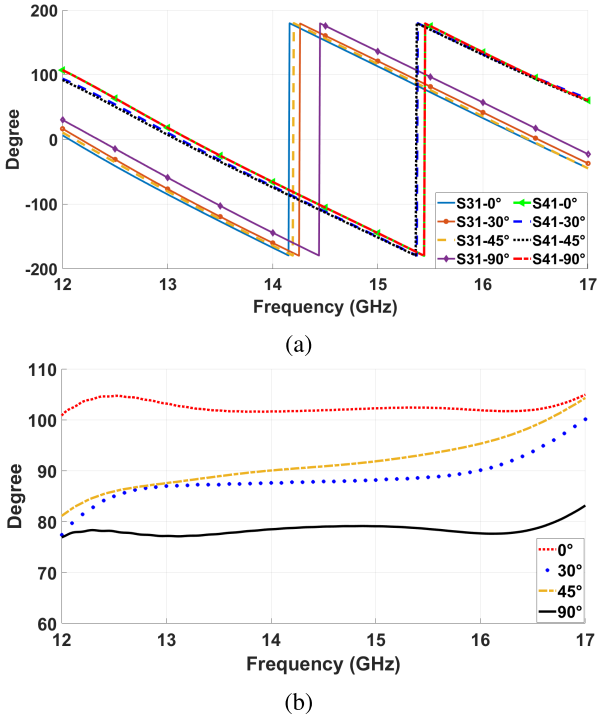

FIGURE 20. Phase variation with angle of rotation a) phase at port 3 and port 4 b) phase difference ($\angle S_{41}$- $\angle S_{31}$).

difference of 105° is attained with the MS at 0° position, while a rotation of 90° achieves the lowest phase difference of 77°. Various rotation angles can be employed to produce different phases in the range from 77° to 105°.

Table 3 provides an extensive comparison of the proposed design with previously reported tunable couplers. Firstly, to the best of the authors' knowledge, our proposed design is the first adjustable phase coupler in the Ku band/mm band ranges. That is why we compare our work with reconfigurable couplers in different frequency ranges. Our work supplies the widest FBW compared to other studies. For example, GW-based hybrid couplers reported in [13], [14], and [15] provide a fixed phase difference. The currently proposed coupler design can provide a narrower phase tuning range in comparison to the previously reported ones [26], [28], [29]. These authors used many varactor diodes to be able to tune the phase. However, using this type of lumped element causes huge losses at high frequencies. The frequency reconfigurable coupler in [22] employed an MS to adjust the frequency however the phase difference was kept fixed. Finally, our obtained results show that the additional insertion loss of the proposed coupler is minimum compared to the other studies. It is maintained within the acceptable range.

IV. CONCLUSION

In this paper, a novel reconfigurable MS-based small UWB hybrid circular coupler is developed utilizing the SIGW technology. To the best of the authors' knowledge, our proposed design is the first adjustable phase coupler in the Ku band/mm band ranges. The findings obtained from the simulation show that phase reconfiguration can be accomplished by rotating the MS around the source coupler's central axis. The proposed design is continuously providing a variable phase difference over a fractional bandwidth of 34.45% between 77° and 105°. It is manufactured using PCB technology and measured using a network analyzer. The findings from simulation and measurement exhibit good agreement. This novel proposed coupler can be best used as a traditional beamforming network. It can also be used for beam steering by changing the rotating angle or the operating frequency. So,

it could be a good candidate for radar applications. Moreover, it could also be used for generating the well Grid Of Beams (GOB) networks. The current design supplies the widest FBW compared to other studies. It is very important to point out that our design provides a simple, easy fabrication and implementation, compact in size, and easy-to-integrate solution with array antennas etched on the top layer of the structure as slot antennas without adding extra PCB materials to construct the antenna array. These novel features are solely comparing our design with all others mentioned in the literature. Also, the amplitude variation can be adjusted to change the beamwidth of the generated beams in the beamforming network. This work is being extended by changing the unit cell material and dimensions in the mm-Wave band.

REFERENCES

[1] M. M. M. Ali and A. Sebak, "Compact printed ridge gap waveguide crossover for future 5G wireless communication system," *IEEE Microw. Wireless Compon. Lett.*, vol. 28, no. 7, pp. 549–551, Jul. 2018.

[2] M. O. Shady and A. M. M. A. Allam, "A novel design of printed ridge gap waveguide-based 0-dB backward-wave coupler," *Int. J. RF Microw. Comput.-Aided Eng.*, vol. 32, no. 11, Nov. 2022.

[3] M. Farahani, M. Akbari, M. Nedil, T. A. Denidni, and A. R. Sebak, "A novel low-loss millimeter-wave 3-db 90° ridge-gap coupler using large aperture progressive phase compensation," *IEEE Access*, vol. 5, pp. 9610–9618, 2017.

[4] E. Nematpour, M. H. Ostovarzadeh, and S. A. Razavi, "Development of a wide band TEM-based Bethe hole coupler using ridge gap waveguide technology," *AEU, Int. J. Electron. Commun.*, vol. 111, Nov. 2019, Art. no. 152933.

[5] D. Shen, K. Wang, and X. Zhang, "A substrate integrated gap waveguide based wideband 3-dB coupler for 5G applications," *IEEE Access*, vol. 6, pp. 66798–66806, 2018.

[6] M. M. M. Ali, S. I. Shams, and A. Sebak, "Ultra-wideband printed ridge gap waveguide hybrid directional coupler for millimetre wave applications," *IET Microw., Antennas Propag.*, vol. 13, no. 8, pp. 1181–1187, Jul. 2019.

[7] S. Birgermajer, N. Jankovic, V. Crnojevic-Bengin, M. Bozzi, and V. Radonic, "Forward-wave 0 dB directional coupler based on microstrip-ridge gap waveguide technology," in *Proc. 13th Int. Conf. Adv. Technol., Syst. Services Telecommun. (TELSIKS)*, Oct. 2017, pp. 154–157.

[8] M. H. Ghaly, M. S. H. S. El-Din, A. M. M. A. Allam, and D. E. Fawzy, "SIGW based bi-directional coupler for Ku-band applications," in *Proc. 9th Int. Conf. Electr. Electron. Eng. (ICEEE)*, Mar. 2022, pp. 36–39.

[9] M. M. M. Ali, M. S. El-Gendy, M. Al-Hasan, I. B. Mabrouk, A. Sebak, and T. A. Denidni, "A systematic design of a compact wideband hybrid directional coupler based on printed RGW technology," *IEEE Access*, vol. 9, pp. 56765–56772, 2021.

[10] M. M. M. Ali, S. I. Shams, and A. R. Sebak, "Printed ridge gap waveguide 3-dB coupler: Analysis and design procedure," *IEEE Access*, vol. 6, pp. 8501–8509, 2018.

[11] M. A. Nasr and A. A. Kishk, "Analysis and design of broadband ridge-gap-waveguide tight and loose hybrid couplers," *IEEE Trans. Microw. Theory Techn.*, vol. 68, no. 8, pp. 3368–3378, Aug. 2020.

[12] Z. Mousavirazi, M. M. M. Ali, H. N. Gheisanab, and T. A. Denidni, "Analysis and design of ultra-wideband PRGW hybrid coupler using PEC/PMC waveguide model," *Sci. Rep.*, vol. 12, no. 1, Aug. 2022, Art. no. 14214.

[13] D. Zarifi and A. R. Shater, "DESIGN of a 3-DB directional coupler based on groove gap waveguide technology," *Microw. Opt. Technol. Lett.*, vol. 59, no. 7, pp. 1597–1600, Jul. 2017.

[14] Z. Zhao and T. A. Denidni, "Millimeter-wave printed-RGW hybrid coupler with symmetrical square feed," *IEEE Microw. Wireless Compon. Lett.*, vol. 30, no. 2, pp. 156–159, Feb. 2020.

[15] M. Taraji and M. Naser-Moghaddasi, "Design of branch line coupler based on ridge gap waveguide technology for X-band application," *IETE J. Res.*, vol. 68, no. 2, pp. 917–923, Mar. 2022.

[16] D. Zarifi, A. Farahbakhsh, and A. U. Zaman, "Design and development of broadband gap waveguide-based 0-dB couplers for Ka-band applications," *IET Microw., Antennas Propag.*, vol. 16, no. 11, pp. 718–724, Sep. 2022.

[17] B. Xu, S. Zheng, and Y. Long, "A phase tunable hybrid coupler with enhanced bandwidth," *Int. J. RF Microw. Comput.-Aided Eng.*, vol. 29, no. 8, Aug. 2019, Art. no. e21779.

[18] H. Peng, P. Lei, H. Yang, S. Zhao, and X. Ding, "Π-type reconfigurable coupler based on a complementary tunable method," *J. Electromagn. Waves Appl.*, vol. 35, no. 12, pp. 1611–1618, Aug. 2021.

[19] H. N. Chu and T.-G. Ma, "Tunable directional coupler with very wide tuning range of power division ratio," *IEEE Microw. Wireless Compon. Lett.*, vol. 29, no. 10, pp. 652–654, Oct. 2019.

[20] U. Shah, M. Sterner, and J. Oberhammer, "High-directivity MEMS-tunable directional couplers for 10–18-GHz broadband applications," *IEEE Trans. Microw. Theory Techn.*, vol. 61, no. 9, pp. 3236–3246, Sep. 2013.

[21] L. Marcaccioli, P. Farinelli, M. M. Tentzeris, J. Papapolymerou, and R. Sorrentino, "Design of a broadband MEMS-based reconfigurable coupler in Ku-band," in *Proc. 38th Eur. Microw. Conf.*, Oct. 2008, pp. 595–598.

[22] Y. Wan, H. Chen, Q. Chen, and Z. Li, "A miniaturized frequency-reconfigurable rat-race coupler based on metasurface," in *IEEE MTT-S Int. Microw. Symp. Dig.*, Jul. 2020, pp. 1–3.

[23] X. Tan and F. Lin, "A novel rat-race coupler with widely tunable frequency," *IEEE Trans. Microw. Theory Techn.*, vol. 67, no. 3, pp. 957–967, Mar. 2019.

[24] B. Dwivedy and S. K. Behera, "Modelling, analysis and testing of an active element based wide-band frequency tunable compact rat-race hybrid," *AEU, Int. J. Electron. Commun.*, vol. 103, pp. 24–31, May 2019.

[25] X. Tan, F. Lin, H. Sun, and Q. Xue, "Planar reconfigurable balanced rat-race coupler with improved amplitude imbalance performance and common-mode noise absorption," *IEEE Trans. Microw. Theory Techn.*, vol. 68, no. 10, pp. 4276–4289, Oct. 2020.

[26] B. W. Xu, S. Y. Zheng, W. M. Wang, Y. L. Wu, and Y. A. Liu, "A coupled line-based coupler with simultaneously tunable phase and frequency," *IEEE Trans. Circuits Syst. I, Reg. Papers*, vol. 66, no. 12, pp. 4637–4647, Dec. 2019.

[27] S. Y. Zheng, "Simultaneous phase- and frequency-tunable hybrid coupler," *IEEE Trans. Ind. Electron.*, vol. 64, no. 10, pp. 8088–8097, Oct. 2017.

[28] H. Zhu and A. M. Abbosh, "A compact tunable directional coupler with continuously tuned differential phase," *IEEE Microw. Wireless Compon. Lett.*, vol. 28, no. 1, pp. 19–21, Jan. 2018.

[29] Y. F. Pan, S. Y. Zheng, W. S. Chan, and H. W. Liu, "Compact phase-reconfigurable couplers with wide tuning range," *IEEE Trans. Microw. Theory Techn.*, vol. 68, no. 2, pp. 681–692, Feb. 2020.

[30] M. S. H. S. El-Din, S. I. Shams, A. M. M. A. Allam, A. Gaafar, H. M. Elhennawy, and M. F. A. Sree, "SIGW based MIMO antenna for satellite down-link applications," *IEEE Access*, vol. 10, pp. 35965–35976, 2022.

[31] I. Afifi and A. R. Sebak, "Wideband printed ridge gap rat-race coupler for differential feeding antenna," *IEEE Access*, vol. 8, pp. 78228–78235, 2020.

[32] Z. Szabo, G. H. Park, R. Hedge, and E. P. Li, "A unique extraction of metamaterial parameters based on Kramers–Kronig relationship," *IEEE Trans. Microw. Theory Techn.*, vol. 58, no. 10, pp. 2646–2653, Oct. 2010.

MOHAMED ATEF ABBAS was born in Egypt. He received the B.Sc. and M.Sc. degrees in electronics and communications engineering from the Arab Academy for Science and Technology and Maritime Transport, Cairo, Egypt, in 2009 and 2014, respectively. He is currently pursuing the Doctor of Philosophy degree in electrical engineering–electronics and communications with Ain Shams University, Cairo, the pre-Ph.D. courses were fulfilled and he is currently preparing the Doctor of Philosophy thesis. He currently works as an Assistant Lecturer with the Arab Academy for Science and Technology and Maritime Transport.

MEHMET FARUK CENGIZ received the B.Sc. degree in electrical and electronics engineering from Eskisehir Osmangazi University, Turkey, in 2013. He is currently pursuing the M.Sc. degree in electrical and electronics engineering with the Izmir University of Economics, Turkey. His main research interests include antenna design, mm-waves, RF and MW technology, and MIMO antenna systems.

A.M.M.A. ALLAM was born in Cairo, Egypt, in 1955. He received the B.S. and M.S. degrees in electrical engineering from MTC and Cairo University, in 1978 and 1985, respectively, and the Ph.D. degree in electrical engineering from Kent University, U.K., in 1988. From 1978 to 1980, he was an Engineer at the Air Force in the Egyptian Army, working in maintenance and repair for airborne equipment in C-130 aircraft, where he was a Crew Member that interval. From 1981 to 1984, he was a Researcher and an Instructor in the Air Born Equipment Department, MTC, Cairo, where he has been a Lecturer and a Researcher, since 1988. He was a Granted Associate Professorship and a Professorship, in 1995 and 2000, respectively. He was the Dean and the Deputy Commandant of the MTC. He was also the Dean and the Vice Dean of the Faculty of Information Engineering and Technology, German University, Cairo. He is the Head of the Communication Department with the German University. He published more than 100 conference and journal papers. His research interests include RF and microwave technology, antenna design, smart antennas for vehicles and radar sensors, satellite communication, and diagnoses of censer based on the electromagnetic properties of human organisms. He did a lot of applied research in RADAR absorbing materials including Chiral, FSS, and textile materials.

DIAA E. FAWZY (Member, IEEE) was born in Egypt, in 1968. He received the Ph.D. degree from Heidelberg University, Germany, in 2001. He was involved for many years in the German GSM-R Project and was responsible for the network planning and optimization. He has been with the Izmir University of Economics, since 2008, where he is currently a Professor and the Head of the Department of Aerospace Engineering. He is a reviewer in many international journals. His current research interests include microwave devices, computational electromagnetics, antennas design, mm-waves, MW technology, remote sensing, and AI.

HADIA M. ELHENNAWY (Member, IEEE) received the B.Sc. and M.Sc. degrees from Ain Shams University, Cairo, Egypt, in 1972 and 1976, respectively, and the Doctorate of Engineering (Dr.-Ing.) degree from the Technische Universität Braunschweig, Braunschweig, Germany, in 1982. Since 1992, she has been a Professor in communication engineering with the Electronics and Communications Engineering Department, Ain Shams University. In 2004, she became the Vice-Dean for graduate study and research. In 2005, she became the Dean of the Faculty of Engineering, Ain Shams University. Her research interests include microwave devices and subsystems, filters and antennas for modern radar, and wireless communications applications.

MOHAMED FATHY ABO SREE was born in Egypt. He received the M.Sc. degree from the Arab Academy for Science and Technology (AASTMT), in 2013, and the Ph.D. degree in electrical engineering from Ain Shams University, Egypt, in 2019. His research interests include antenna design and MW technology. He is reviewing in IEEE Access and *PIER* on-line journal.